Chapter 2

Simulation of convective detonation waves in a porous medium

Peculiar detonation-like flows in rigid porous media were observed in [73–78]. The active component of such media can be a gas mixture that fills pores [73] or a layer of a high explosive (HE) on the pore surface [78] or a fuel film [74–77].

The wave regimes of combustion in a rigid porous medium are characterized by a complex wave front, which is a random pulsating relief of hills and valleys, and by a smooth increase in pressure. The average front velocity is ≈ 1 km/s. The front pattern and the pressure profile are shown schematically in fig. 2.1.

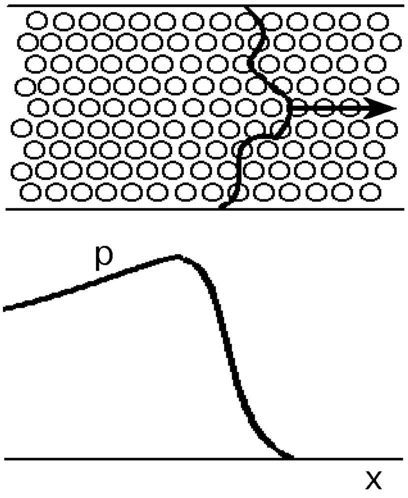

Figure 2.1.

In opinion of authors of experimental works, the waves propagate by a convective or jet mechanism. The wave-propagation conditions are strongly affected by the porous bed. Because of friction losses, the wave velocity is not sufficient to initiate a reaction by the standard shock-wave mechanism. Instead, ignition is ensured by hot gas jets that burst ahead of "average" front from the combustion zone.

Previously, similar conclusions were made for a different system — a porous explosive [79, 80]. Some initiation regimes, such as an electric discharge or explosion of a conductor inside HE, injection of hot combustion products from a separate chamber upon rupture of a membrane or the action of gas-detonation products on a powder, also generate a wave with a velocity of ≈ 1 km/s and a pressure of ≈ 2 kbar. In charges of small diameter (3–4 mm) with a very light shell, this wave is rather stable; here a smooth increase in pressure and formation of jets were also observed. Although the low strength of HE leads to slight deformation of the porous bed, available data also suggest a jet mechanism of wave propagation. From the pressure level, the burnt fraction of the material is estimated at several percent, i.e., the concentration of the reacted HE is close to that used in the experiments of [78].

In this work, we consider a system in which a gaseous oxidizer in pores reacts with a fuel film on the surface of the pore structure [74–77]. Physically, an active porous medium of the "gas–film" type can be, for example, sand or packing of rigid granules, with pore walls covered by a thin film of fuel that can react with pore-filling oxidizer. The initiation of such a system is possible by the "shock" of a gas detonation.

2.1 Discrete model of convective wave

The flow of gas was simulated by the LGA method (see chapter 1). For flow in a porous medium, the drawbacks of this model are insignificant because the flow velocity is low due to friction. Of course, simulation of fast jets can be only qualitative, but today this is true for deterministic finite-difference methods. Some results of application of the isothermal FHP lattice model to the problem of convective waves are reported in [81, 82]. These papers deal with the case of "isothermal detonation", where the active component is an explosive. In this case, the temperature of the gas (reaction products) in the combustion zone is constant.

For gas-film detonation in the reaction zone, the temperature is obviously variable. It increases during fuel burnup from the low initial temperature of the oxidizer to the temperature of combustion products. It is clear that the isothermal FHP model is inapplicable to this system.

Therefore, we implemented a nine-velocity version of the method on a square lattice [20], which is schematically shown in fig. 1.3. Particles move along the sides of the square (density n_1, velocity 1, and energy 1/2) or its diagonals (density n_2, velocity $\sqrt{2}$, energy 1). Each of these eight states can be occupied by one or none particle. In addition, there are rest particles (density n_0), whose number may in principle be arbitrary (in our computations, it is not more than six). The system simulates a two-dimensional gas with density $\rho = n_0 + n_1 + n_2$ and pressure $p = n_1/2 + n_2 - \rho u^2/2$. The presence of three "energy levels" makes it possible to introduce a variable temperature $T = p/\rho$. The "diagonal" particles correct to some extent the disadvantages of the square lattice by producing nondiagonal components of the momentum flux.

A standard lattice step in time includes propagation of particles to neighbor nodes and collisions at nodes. The result of collision is chosen randomly out of all possible states that have the same number of particles, momentum, and energy and are not identical to the initial state (when present). A table of possible states is calculated before computation. Some examples of collisions are shown in fig. 1.3.

A gas-dynamic block (propagation + collision) was tested in special computation. Averaged values of the momentum flux tensor Π_{ik} were calculated for specified equilibrium states. They were close to $p\delta_{ik}$ — the main term. The inertial terms were of the order of $\rho u_i u_k$, although the coefficients depended significantly on the distribution of particles over the levels (i.e., on the temperature). For flow in a porous medium, the error in describing these components, which are quadratic in velocity, is insignificant because the velocity is low due to friction (~ 0.1).

In addition, a velocity of propagation of small perturbation over a homogenous state was determined. In the range studied, the propagation velocity of a "step" perturbation was nearly constant (between 0.9 and 1, although the temperature in test computations varied by at least an order of magnitude. This is a consequence of the inaccuracy of the model, namely the limited number of possible states.

A decrease in temperature (achieved by the prevalence of rest particles) did not lead to a noticeable decrease in wave velocity because perturbations were transferred by moving particles, whose velocity along the lattice axes is equal to unity. An "ideal" dependence $c = \sqrt{2P/\rho} \sim \sqrt{T}$ might be expected for very long waves when the flow has a chance to attain local thermal equilibrium. For the problem considered, such waves are of no interest.

A complete cycle of computation ignoring heat losses consists of four steps. Along with propagation and collisions, it includes a reaction and friction against the porous bed. Combustion was simulated by introducing two sorts of gas particles: "blue" particles (oxidizer) and "red" particles (combustion products). Initially, the pores contain only the oxidizer. Fuel (which forms a film on the pore walls in the physical system) participate in the computation as a source of particles that "evaporate" into the gas. In the simplest case, the reaction at each node involves formation of two high-energy "red" product particles from one rest "blue" particle and one fuel particle. "Red" particles cannot turn into "blue" particles (the reaction is irreversible) but "red" and "blue" particles can exchange energy during collisions. This simulates the process

$$A + B \longrightarrow 2C$$

with the energy effect equal to 2. At a given node, combustion begins when a certain condition is satisfied (for example, upon reaching specified temperature and pressure averaged over the nearest neighborhood of the given node) with given probability of the reaction w. For each node, once combustion began, the ignition condition was not further verified. This corresponds to the irreversibility of ignition in a given pore.

Reaction at the "burning" node occurs with the same probability w. The introduction of this parameter reflects to some extent the nonuniformity of the sizes and geometry of real pores, which should affect ignition and combustion. In most computations, we used the value of $w = 0.5$. Naturally, for the reaction, it is necessary that unexpended fuel, oxidizer, and two free diagonal states be present at a given node.

If three or four free diagonals were available, three diagonal product particles were formed (reaction $A + 2B \longrightarrow 3C$) from one fuel particle and two rest oxidizer particles (naturally, if they were present). This improves the stoichiometry because conventional fuel (for example, of gross-composition CH_2) is markedly lighter than the oxidizer ($1.5O_2$). For four free diagonals, new particles were randomly directed.

The last step of the cycle simulated friction. In the range of interest to us, the friction force is proportional to the squared velocity:

$$\mathbf{f} = -k\frac{\rho u \mathbf{u}}{d},$$

where d is the particle size of the porous bed and k is the friction coefficient. According to [83], $k = 1.75(1-\varphi)/\varphi^2$, where φ is the porosity (about 0.4 for loose packing). According to more recent data [84], the friction coefficient is approximately half the indicated value. Therefore, we assumed $k = 3.5$.

To use the friction law in the discrete system, we consider the deceleration of gas in one time step. For spatially uniform case, one can write $\rho \partial u/\partial t = f$, which leads to

$$\frac{du}{u^2} = -k\,dt\,.$$

Integrated over time interval τ, this equation results in

$$\Delta u = u(\tau) - u = -\frac{\tau k u}{d + \tau k u}.$$

This deceleration would be achieved on average, if we introduce the probability of velocity change

$$w = \frac{|\Delta u|}{u} = \frac{\tau k u}{d + \tau k u}.$$

The velocity at each node should be put to zero with the probability w. For each node, we calculated the local flow velocity u (averaged over nine points — a node and eight nearest neighbors). Then, the state at the node was replaced with probability $w = \tau ku/(d + \tau ku)$ by a new one with the same number of particles and the same energy but a random value of the momentum, so that, on the average, the velocity in the new state became zero. This procedure simulates loss of momentum in quadratic friction in time step τ. At the same time, the stochasticity of flow in a porous medium is simulated. The time step τ was always considered unit. In most of the computations, $d = 1$.

2.2 Computation results

Although the computations were performed in dimensionless form, it is conveniently to assume that the lattice spacing is 1 mm and the time step is 1 mks. The velocity is then expressed in km/s. For the density, any scale can be adopted, and the pressure is then expressed in the units of ρu^2. For example, if the unit of density corresponds to 10^{-3} g/cm^3 = 1 kg/m^3, the unit of pressure is 1 MPa. For temperature, the reasonable coefficient of conversion can correspond to 3000 K per unit.

We used a lattice with $1 \le x \le 250$ and $1 \le y \le 125$. On the top and bottom boundaries, periodic boundary conditions were imposed, and the right and left boundaries were rigid walls. Initial concentrations of the fuel f and oxidizer ("blue" particles) were specified: in the standard version, $f = 1.5$, $n_0 = 3$, $n_1 = 0.8$, $n_2 = 0.32$. Moving particles were distributed according to the probability of occupation. For the rest particles and the fuel (n_0 and f), the integer part was first distributed uniformly, and the fractional part, when present, was then randomly distributed. After several collisions, equilibrium was established in the gas. The initial concentrations are close to the equilibrium values corresponding to the specified density and energy.

Then, combustion was initiated by specifying a hot region with larger values of $n_1 = 1{,}2$ and $n_2 = 0{,}96$ for $x < 7$ (which corresponds to an increase in pressure by a factor of 2.17 and an increase in temperature by a factor of 1.73). At an ignition temperature of 0.4, a threshold pressure of 2.1, and a probability of reaction of 0.5, this perturbation developed into a quasistationary wave that "forgot" the initial conditions. An example of computation is shown in fig. 2.2.

The wave is obviously nonuniform, especially at the beginning. This is a consequence of the randomness in the initial conditions. At $t = 50$, the hot region looks like two "peninsulas". In fact, because of vertical periodicity, this

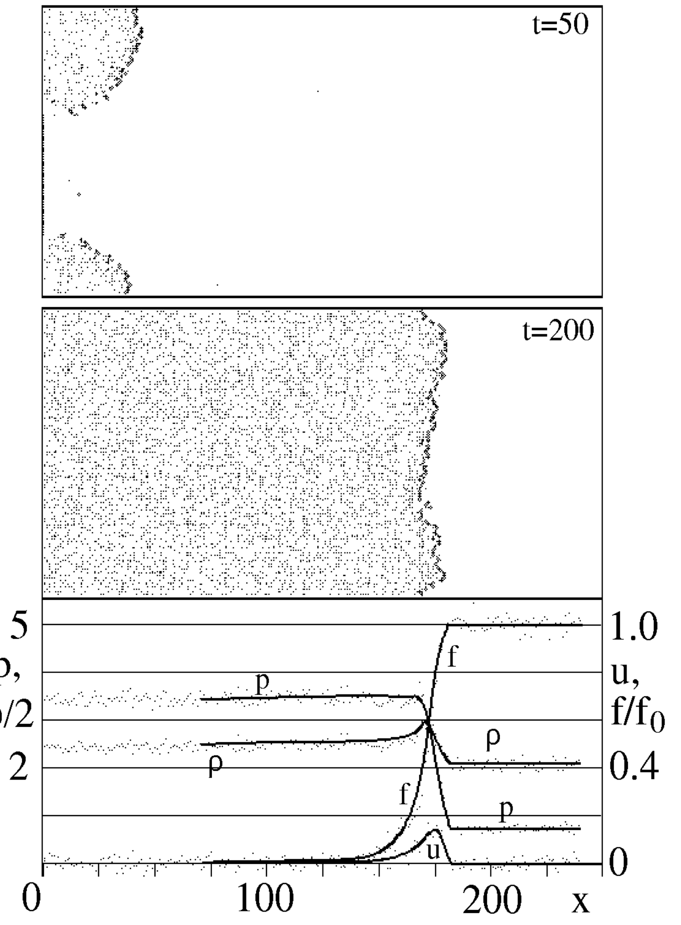

Figure 2.2. Position of the wave front (ignition sites) and qualitative distribution of local pressure for various times after the beginning of propagation: nodes at which $p > 4$ are shown, and for the last time, the averaged wave structure is presented

is one hot zone. The front is later smoothed but even after attainment of a quasistationary regime, it does not become completely flat. At the bottom of the figure there are plots of pressure, fuel concentration, density and velocity averaged over the vertical coordinate[1] (for example, $\langle p(x)\rangle = \sum\limits_{y=1}^{125} p(x,y)/125$). For the given kinetics, the increase in the average pressure is smooth and corresponds to the region over which the wave front "is smoothed".

The average wave velocity was measured from the shift of the pressure profile from the time $t = 100$ and at $t = 200$, it was 0.93 km/s (in natural units), which is larger than the perturbation velocity in the initial state (0.9) but smaller than that in products (1.0). This corresponds to experiments with the only difference being that in the lattice gas, the range of sound velocities is very narrow. The flow velocity, as noted above, is about 0.1.

The increase in density corresponds to injection of fuel. At the wave front there is a small peak due to local compression.

As the probability of reaction w increases to 1, a flatter wave front is obtained; accordingly, the pressure rise is sharper. The wave velocity is $D = 1.19$.

---

[1] Letters p, u, ρ and f in fig. 2.2–2.4 denote the corresponding curves, and the scaled quantities $\rho/2$ and f/f_0 are laid on the vertical axis.

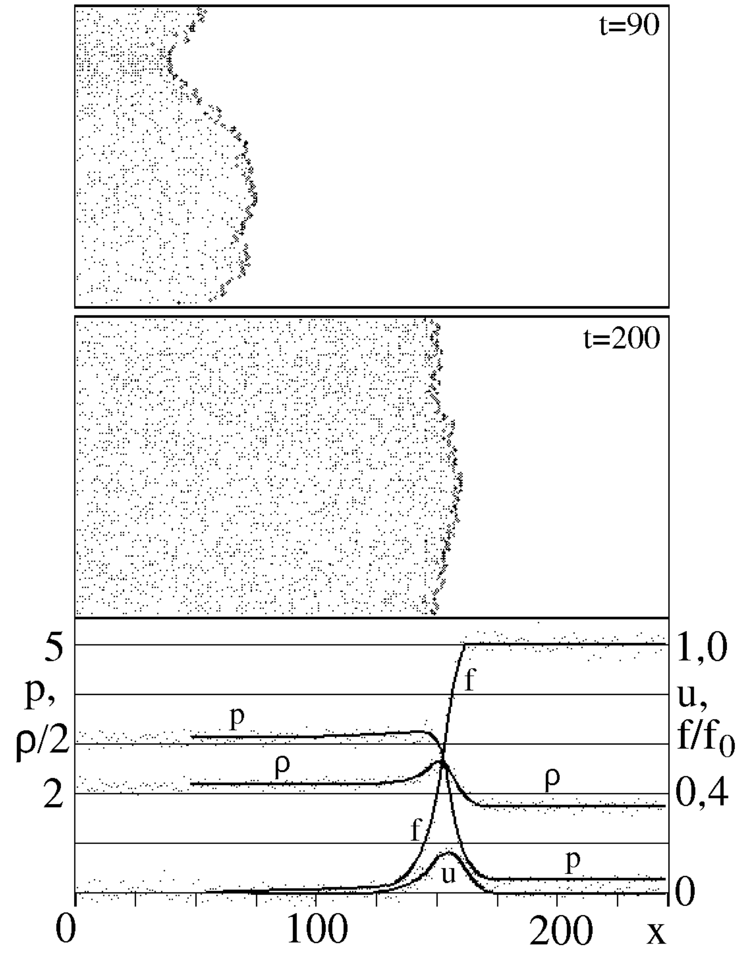

Figure 2.3. Slow wave at low initial temperature

Hence, the wave is supersonic with respect to both the cold initial gas and reaction products. In further computations, we set $w = 0{,}5$.

Figure 2.3 shows the results for a colder initial state with temperature half that used in the previous computations. Here the front is also significantly irregular and the wave velocity is equal to 0.78, which is less than the velocity of sound in the initial state. As a result, there is a certain increase in pressure and velocity ahead of the ignition front. The gas has managed to lead the slow combustion wave. This may be a source of some nonstationarity. The gas ahead of the front favors faster ignition and acceleration of the wave front. However, because of large friction, the penetration effect is slow, and in the computational domain, acceleration was not observed.

2.3 Effect of heat losses

In experiments there is a heat flow from the reaction mixture to the porous bed, which leads to cooling of the gas. Elaboration of the lattice model allows this effect to be taken into account. The scheme is supplemented with a fifth step

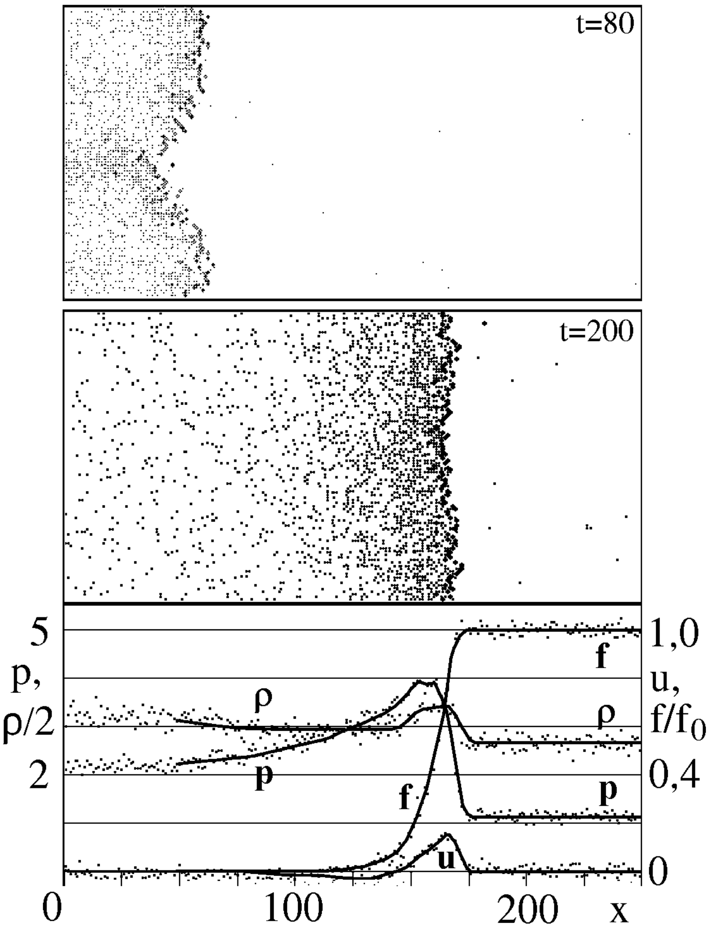

Figure 2.4. Combustion wave in the presence of heat losses

— computation of heat losses. The heat flux (per unit volume of the pores) was calculated from the formula

$$q = \frac{6(1-\varphi)}{d} \cdot \frac{\kappa(T-T_0)}{\varphi d} \cdot \mathrm{Nu},$$

where d is the particle diameter, κ is the thermal conductivity of the gas, T_0 is the initial temperature, and Nu is the Nusselt number. The standard Denton relation was used [85]: $\mathrm{Nu} = 2 + 0{,}6 \cdot (\rho u d\varphi/\eta)^{0{,}7}$, where η is the dynamic viscosity of the gas. At each node, the heat losses q was calculated in dimensionless units. Then, the energy at a node was decreased by two units with probability $q/2$, which simulates the heat loss per unit step in time. The mass and momentum were not affected.

The computation results are shown in fig. 2.4. The initial pressure (1 MPa) and particle size of the porous medium (2.5 mm) are the same as in [75]. In the computation, the initial density was 5.3 kg/m^3 (2.5 times lower than in [75]). The difference in density results from the inaccuracy of the model. It is not significant because the main dependences are easily scaled (the pressure rise, for example, is nearly proportional to density). An exception is heat exchange ($q \sim \rho^{0.7}$, and the energy in unit volume is proportional to ρ). Because of the decreased density, cooling in the computation is accelerated by approximately 30%, which can be neglected taking into account the qualitative character of the computation model. Thus, the effect of density is also insignificant for heat exchange.

The computed wave velocity (925 m/s) is close to the experimental value (940 m/s). The pressure profile shape is also in qualitative agreement with measurements [75]. The agreement of the pressure rise time suggests a reasonable choice of the kinetics and the agreement of the pressure decrease indicates that the heat exchange was properly taken into account.

We note that the experimental and computed pressures agree only in order of magnitude. This difference is partly related to the lower initial density but even after multiplication of the computed pressure by 2.5 — the ratio of the experimental and computation densities — a difference of about three times remains. This is of course a consequence of the inaccuracy of the model. Because of the discrete nature of the processes and the stiff bounds for the main constants, it is impossible to simultaneously obtain agreement for wave velocity and amplitude.

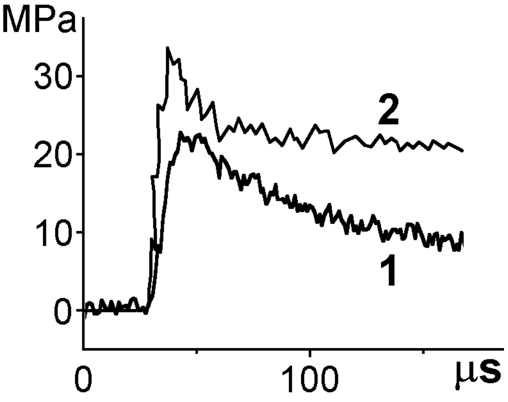

Figure 2.5. Curves of $p(t)$ for the present computation (1) and the experiment of [75] (2)

A better agreement is achieved by correcting the model and recalculating the results using reasonable physical considerations. Let us consider the difference in the properties between the real and lattice gases. The real adiabatic exponent of the combustion products is $\gamma \approx 1.3$, and the energy release per unit mass of the products is $Q \approx 11$ kJ/g. For the lattice model, $\gamma = 2$ and $Q = 1$ kJ/g (in the adopted units). The reaction proceeds in a practically constant volume, and the final pressure is $P \approx (\gamma - 1)\rho Q$. For a real fuel of stoichiometric composition, the final density is $\rho \approx 1.3\rho_0$, and in the computations presented in fig. 2.4, $\rho \approx 1.5\rho_0$. With equal initial density of the oxidizer ρ_0, the model should give a pressure about three times lower than that in the real process.

Figure 2.5 gives curves of pressure versus time. Curve 1, showing the average pressure in a certain cross section, is calculated from the data of fig. 2.4, and curve 2 is an experimental curve taken from [75]. The initial pressure in the computation is subtracted to simulate a piezoelectric gauge record. The computed pressures are increased by a factor of 7.5 to compensate for the differences in thermodynamics and stoichiometry (coefficient 3) and initial density (coefficient 2.5). After this recalculation, quantitative results of modeling practically coincide with the experiment. We note that the heat exchange is overestimated by approximately 30%, which explains in part faster decrease in computed wave pressure. The residual difference has the same order of magnitude as the experimental scatter. This agreement is even better than one might expect for the model considered. Thus, the comparison performed shows that the lattice model gives a reasonable description of the process.

The computations show a qualitative agreement with the experimental picture of the phenomenon. The wave generally has an irregular front, whose bulges should be identified with the initiating jets. The protrusion at the front where the reaction begins and the pressure increases tends to propagate further. In contrast, friction and lateral expansion of the protrusion stabilize the front. The interaction of the randomness, gas dynamics, and dissipation determines the front shape.

The wave velocity is close to the velocity of sound. The jet mechanism suggests exactly this order of magnitude for the average velocity of the front [86]. However, in wave computation by the continual model, one has to specify the velocity of the front. In the discrete model with specified kinetics, the motion of the front is obtained automatically. This, along with simulation of the complex front shape, is among the unquestionable advantages of the discrete method. We note that supersonic (relative to the products) waves are qualitatively similar to subsonic waves because of friction, which quenches gas-dynamic perturbations [86]. Generally, the regimes obtained can be considered as intermediate between combustion and detonation.

The flow velocity is about an order of magnitude lower than the wave velocity. This, as well as the general wave structure, is in good agreement with the results of the simplified continual model of [86]. We note that in the discrete model, friction is quite real, thus describing the most important feature of the wave — stagnation of average flow. At the level of mechanics, the ”short model” [86] is supported by direct computations. The heat exchange in the model is also real (to an extent to which it is possible to use the notion of temperature).

At the same time, the model is rather crude. Because of the small number of energy states, the temperature of the lattice gas is limited (not more than 1). For a more accurate simulation of the large temperature and pressure gradients (by several tens times), one need to assign an initial state with a temperature of about 0.01, i.e., a state that practically consists of rest particles. The physical meaning of such formulation is questionable.

Summary

The lattice method is useful for modeling the mechanics of the process, because, first of all, it takes into account fluctuations and randomness at the mesoscale (pore size). Usually, statistical noise is regarded as a shortcoming of lattice computations but in the present problem it is vital. Waves with a reaction in crowded space is an almost ideal object for the lattice approach.

At the same time, the lattice gas is a qualitative method with respect to kinetics and thermodynamics. At present, however, due to the inaccuracy of available experimental information there is little point in more refined approaches. We believe that there is no ideal computational method and it is most reasonable to combine discrete and continual approaches.